

## Transport and Turbulence with Innovative Plasma Shapes in the TCV Tokamak

B. Labit 1), A. Pochelon 1), M. Rancic 1), F. Piras 1), A. Bencze 1), A. Bottino 2), S. Brunner 1), Y. Camenen 3), P.K. Chattopadhyay 4), S. Coda 1), E. Fable 2), T.P. Goodman 1), S. Jolliet 5), A. Marinoni 1), L. Porte 1), B.F. McMillan 1), S. Yu. Medvedev 6), O. Sauter 1), V. S. Udintsev 7), L. Villard 1), and the TCV Team

1) Ecole Polytechnique Fédérale de Lausanne (EPFL), Centre de Recherches en Physique des Plasmas, Association EURATOM-Confédération Suisse, CH-1015 Lausanne, Switzerland

1) Max-Planck-Institut für Plasmaphysik (IPP) Boltzmannstraße 2, Garching, Germany

2) CSFA, Dpt. of Physics, University of Warwick, Coventry, UK

3) Institute for Plasma Research, Bhat, Gandhinagar, Gujarat, India

4) Japan Atomic Energy Agency, Higashi-Ueno 6-9-3, Taitou, Tokyo 110-0015, Japan

5) Keldysh Institute of Applied Mathematics, Russian Academy of Sciences, Moscow, Russia

6) ITER Organization, 13108 Saint-Paul-Lez-Durance CEDEX, France

email contact of main author: benoit.labit@epfl.ch

**Abstract:** We present recent results on turbulence measurements in TCV L-mode plasmas. It has been shown that the heat transport is reduced by a factor of two for a plasma at negative triangularity compared with a plasma at positive triangularity. This transport reduction is reflected in the reduction of the temperature fluctuation level, in the low frequency part of the spectrum (20-120 kHz), measured by correlation ECE in the outer equatorial plane. Nonlinear gyrokinetic simulations predict that the TEM turbulence might be dominant for these TCV plasmas. The TEM induced transport is shown to decrease with decreasing triangularity and increasing collisionality. Both dependences are in fairly good agreement with experimental observations. We also report on an innovative divertor magnetic configuration: the snowflake (SF) divertor whose properties are expected to affect the local heat load to the divertor plates in particular during ELMs when compared with the classical single-null (SN) divertor. In L-mode plasmas, the intermittent particle and heat transport in the SOL is associated with the presence of "blobs" propagating in the radial direction. Intermittency is compared between SN and SF configurations by looking at the statistical properties of the ion saturation current  $J_{\text{sat}}$  measured with Langmuir probes (LPs) in the LFS scrape-off layer. For ELMy H-mode SF plasmas, the time evolution of  $J_{\text{sat}}$  during ELMs is estimated with LPs covering the strike-points target zones.

### 1. Introduction

In a fusion reactor based on magnetic confinement, the energy transport in the plasma core has to be minimized in order to increase the energy confinement time to values that will satisfy the Lawson criterion. At present, the core transport exceeds the transport due to collisions by at least one order of magnitude and the excess is attributed to turbulence. Therefore it is crucial to know which instabilities create this turbulent state and to find ways to control them and to reduce the induced transport. In L-mode plasmas obtained in the Tokamak à Configuration Variable (TCV,  $R/a = 3.5$ ,  $B_t < 1.54$  T), the energy confinement time increases when the plasma triangularity  $\delta$  is decreased [1]. Dedicated experiments [2] have shown that the mid-radius electron heat diffusivity significantly decreases with decreasing triangularity and, for similar plasma conditions, only half of the ECRH power is required at  $\delta = -0.4$  compared with  $\delta = +0.4$  to obtain the same temperature profile. The electron heat transport level exhibits a continuous decrease with decreasing triangularity and increasing collisionality. These experimental results have motivated global linear gyrokinetic simulations [2]. For all plasma triangularities and toroidal wave numbers, local and global linear simulations indicate that the so-called trapped electron mode (TEM) is the dominant instability and the electron contribution to the total growth rate  $\gamma$  is more than 90%. The maximum transport level, estimated from the mixing length heat diffusivity is obtained for a toroidal mode number  $n \approx 10$  and the heat diffusivity decreases significantly towards negative triangularities for  $n < 10$ . Moreover, nonlinear flux tube simulations show for both linear and

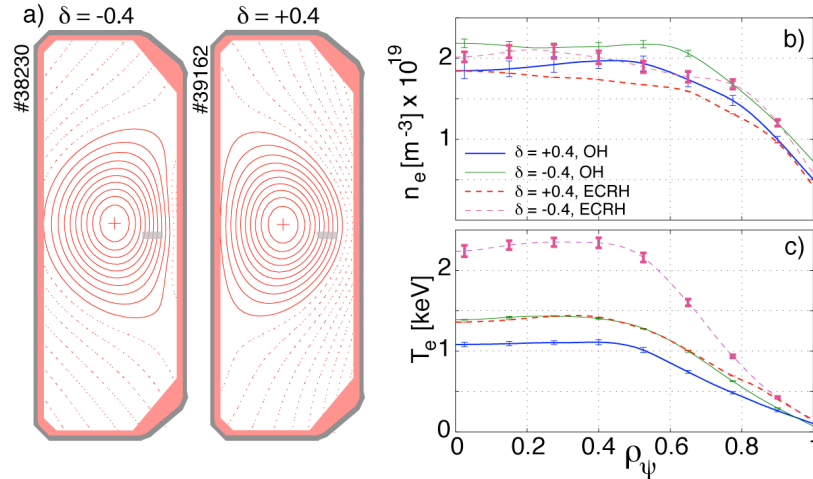


FIG. 1: a) Examples of TCV plasma shapes for negative and positive triangularity; the grey shaded area indicates the measurement location; b) density and c) temperature profiles for the four investigated cases.

nonlinear phases that negative triangularity is found to have a stabilizing influence on ion-scale instabilities, specifically on TEM. Moreover, the variation of the heat flux with triangularity calculated by the nonlinear simulations is in fair agreement with the experimental results. The resulting stabilization is the consequence of a rather complex modification of the toroidal precessional drift of trapped particles exerted by negative triangularity [3]. However, the stabilizing effect of the negative triangularity does not penetrate as deeply in the plasma than found experimentally from the power balance heat diffusivity. These numerical results have motivated our recent measurements of turbulence in the TCV tokamak when the plasma triangularity is significantly varied.

In contrast to the core plasma, transport at the plasma edge has to be optimally distributed to handle power exhaust, to prevent ashes accumulation and to contain plasma-wall interactions to a level that can be tolerated by wall materials. Different solutions have been proposed to reduce the plasma-wall interaction by acting on the magnetic field topology to optimize the divertor action. One of these innovative solutions is the so-called snowflake (SF) divertor [4,5]. In a SF divertor configuration, both the poloidal magnetic field and its spatial first derivatives vanish at the null point. The separatrix divides the poloidal plane in six regions and, as a consequence, the configuration has four divertor legs. Compared to a Single-Null (SN) configuration, the snowflake configuration is characterized by a larger flux expansion around the null point, a longer connection length in the Scrape-of-Layer (SOL) and a larger magnetic shear close to the separatrix. These properties are expected to affect the local heat load to the divertor plates in particular during Edge Localized Modes (ELMs). In Section 2, measurements of temperature fluctuations based on correlation ECE technique are reported for different shapes in TCV L-mode plasmas. First results on the characterization with Langmuir probes of snowflake diverted plasmas in TCV are presented in Section 3. Section 4 concludes the paper.

## 2. Turbulence level measurements with different plasma shapes in TCV

### 2.1 Experimental setup

In the present work, plasma turbulence is investigated with the Electron Cyclotron Emission (ECE) correlation diagnostic. It is built as a separate block of the 24-channels heterodyne

radiometer covering the range 65 to 99 GHz and operating in the second-harmonic extraordinary (X)-mode with the single-side band receiver scheme. It measures the ECE radiation perpendicular to the magnetic field from the LFS with a line of sight at  $z=0$ . Further details of this diagnostic can be found in Ref. [6]. It provides a good tool for electron temperature fluctuations measurements in regions where the plasma is optically thick, i.e. when the optical depth is typically larger than 2. In that case, the plasma behaves like a black body and the ECE is proportional only to the plasma temperature according to  $S_{ECE}(t) = C[\bar{T}_e + \tilde{T}_e(t)][1 + \tilde{N}(t)]$  where  $C$  is a constant factor and  $\tilde{N}$  is the thermal noise due to photon statistics. In situations where two ECE sample volumes are separated in the frequency space, thermal noise decorrelation occurs, which allows for thermal plasma fluctuation measurements provided the correlation length is larger than the sample volume separation. The minimal frequency separation, determined by the sum of each channel bandwidth is  $\Delta f = 0.2$  GHz. Under these conditions, the cross-spectral density  $S_{12}(f)$  between both signals is directly proportional to the relative temperature fluctuations:  $(\tilde{T}_e/\bar{T}_e)^2 \propto S_{12}(f)$ . The sensitivity of the measurement is given by the level of statistically meaningful information that can be extracted from the correlation function, which is set by  $\varepsilon(s_{12}(f)) = \sigma_1\sigma_2/\sqrt{N}$  where  $\sigma_i$  is the standard deviation of the  $i$ -th signal, and  $N$  is the number of independent samples. For typical discharge durations in TCV, the sensitivity yields values below 1%. Such equation often overestimates the experimental noise level, but it can be taken as an upper limit of the diagnostic sensitivity. Limited L-mode plasmas ( $I_p=250$  kA,  $\kappa=1.5$ ,  $q_{\text{edge}} \approx 4$ ) at different triangularities  $\delta = \pm 0.4$  are investigated in the present work (Fig. 1. a)). At the half discharge duration, 580 kW of ECRH power are injected in the plasma by 3 X2 gyrotrons. The absorption is located around  $\rho_{\psi} = 0.65$ , just outside the  $q=1$  surface ( $\rho_{\psi,q=1}=0.6$ ). Thomson scattering profiles of the density and electron temperature are shown in Fig. 1. b-c). The improved confinement at negative triangularity is clearly visible on the  $T_e$  profiles: with ECRH,  $T_e(0)$  increases by  $\sim 60\%$  for  $\delta=-0.4$  and only by 30% for  $\delta=+0.4$ . Moreover, the added ECRH power for the  $\delta>0$  plasma gives a similar  $T_e$  profile compared with the ohmic phase for the  $\delta<0$  plasma. For a fruitful comparison, the requirement of

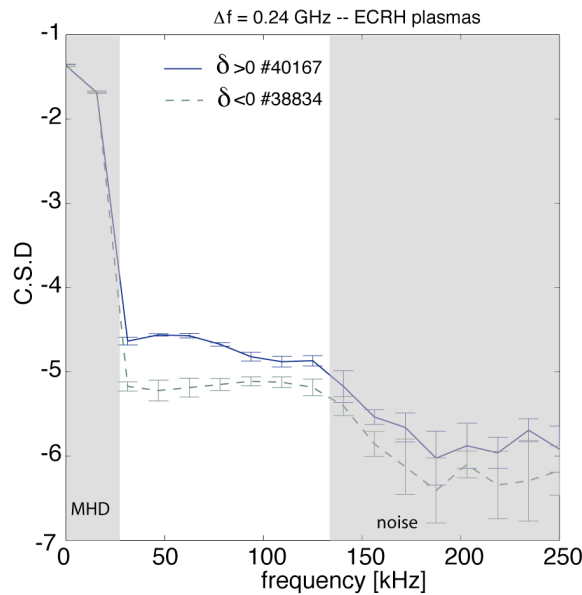


FIG. 2: Cross-spectral density between 2 signals separated by  $\Delta f = 0.24$  GHz for ECRH plasmas. The spectral range of interest is  $20 < f < 80$  kHz.

identical profiles for both triangularities is important since it gives similar values of the gradient characteristic lengths and of the effective collisionality  $\nu_{\text{eff}}$ . Indeed,  $\nu_{\text{eff}}$  is a key parameter for the transport associated with TEM turbulence [2, 3].

## 2.2 Temperature fluctuations measurements and radial correlation length

On a shot-to-shot basis, correlation ECE measurements are performed at  $\rho_{\psi}=0.75$  for several frequency separations ranging from 0.24 GHz to 1.5 GHz for both triangularities. The acquisition frequency is set to 1 MHz and the analysis is done for 500 ms long time series. Cross Spectral Density spectra estimated for  $\Delta f=0.24$  GHz are shown in Fig. 2 for ECRH plasmas with both triangularities. The low frequency part (below 20 kHz) of the spectrum is the typical spectral range of coherent MHD activity. Moreover the spectrum above 120 kHz corresponds to the diagnostic power sensitivity limit. The turbulence frequency range of interest is in between these two limits. It is observed that for similar amount of power injected in the plasma, the level of turbulence is larger for positive triangularity in particular for frequencies below 80 kHz. The relationship between frequency separation and radial separation is given by  $\Delta r = \pi R m_e / (e B_{\phi}) \Delta f$  where  $m_e$  is the electron mass,  $e$  is the elementary charge and  $B_{\phi}$  is the value of the toroidal magnetic field at the position  $R$  in the plasma. The cross-spectral density  $S_{12}(f)$  between both ECE signals is computed for each  $\Delta r$  and its integral over the frequency range of interest is evaluated:  $I_{12} = \int_{20 \text{ kHz}}^{80 \text{ kHz}} S_{12}(f) df$ . In Fig. 3 is reported on a logarithmic scale,  $I_{12}(\Delta r)$  as a function of  $\Delta r$  for the  $\delta > 0$  plasma with ECRH. The integral of the CSD decays exponentially with  $\Delta r$ . One can therefore fit this decay with  $I_{12}(\Delta r) \propto \exp(-\Delta r / \lambda_r)$ , the correlation length  $\lambda_r$  being defined as the e-folding length of the fit. A correlation of about 1 cm is found in this case. A similar analysis for  $\delta < 0$  ECRH plasmas was not possible with our experimental dataset. This is due to the fact that for a radial separation larger than 0.5 cm, ECE signals are almost uncorrelated. The fact that the CSD is

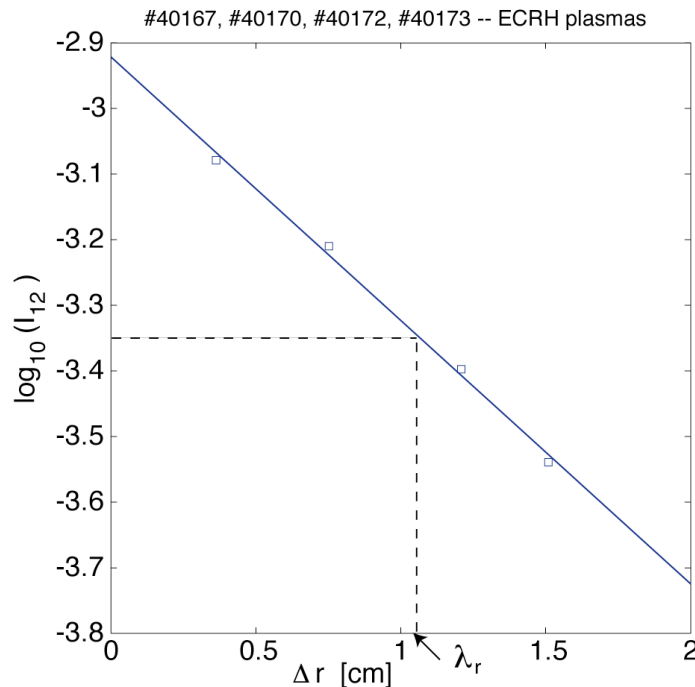


FIG. 3: Exponential decay of the integral of the cross-spectral density over the frequency range of interest ( $20 < f < 120$  kHz) as a function of radial separation for the four investigated cases.

larger in absolute value for  $\delta > 0$  (Fig. 2) is an indication that the turbulence level is higher or the correlation length is longer, or both. Further experimental work and analysis are under way. A comparison of the present experimental findings will be done with a synthetic diagnostic mimicking correlation ECE measurements for the level of fluctuations in nonlinear global gyrokinetic simulations, which are under way.

### 3. Characterization of snowflake diverted plasmas in TCV with Langmuir probes

#### 3.1 Intermittent transport in the SOL for L-mode plasmas with a snowflake divertor

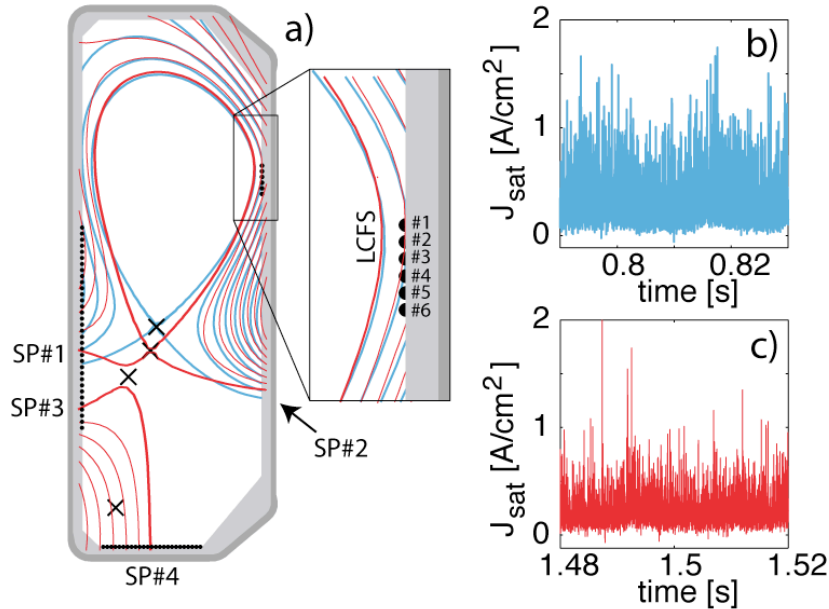


FIG. 4: a) Plasma shapes for the SN (blue) and SF+ (red) configurations with LPs #1-#3 in the SOL. The numbering of the different strike points (SP) is indicated. Examples of measured  $J_{\text{sat}}$  in the SN phase b) and later in the SF+ phase c).

In L-mode plasmas, the intermittent particle and heat transport in the SOL is associated with the presence of "blobs" propagating in the radial direction. Intermittency is compared between SN and SF configurations by looking at some statistical properties of  $J_{\text{sat}}$  fluctuations measured with Langmuir probes (LPs) in the SOL at the LFS midplane. The TCV LP system [7] consists of three single probe arrays installed on the central column (CC) wall, on the floor and on the LFS wall. Probes on the CC wall and on the floor are used to measure  $J_{\text{sat}}$  in the divertor target zones covering the strike points #1, #3 and #4 (see Fig. 4. a)). Here we are focusing on L-mode ohmic plasmas with a single null X-point phase followed within the same discharge by a SF+ phase. A particular care has been paid for the vertical positioning of the plasmas in order to have the three highest LFS LPs in the SOL and not in the private flux region (Fig. 4. a)) as it was the case for plasmas discussed in [8]. The radial distance between the last close flux surface (LCFS) and the Langmuir probes is about 2 cm. Probes are biased at a negative voltage of -80V and therefore measure the ion saturation current which, divided by the effective probe area gives  $J_{\text{sat}}$ . Figure 4 b-c) displays  $J_{\text{sat}}$  measured on LP#2 for both plasma phases (SN and SF+). The nature of intermittent transport is clearly visible with large spikes in  $J_{\text{sat}}$  associated with density blobs propagating radially towards the wall. In order to investigate the influence of the plasma collisionality on the intermittent transport, a density scan is performed. Moments of order 0 (mean), order 1 (standard deviation), order 2 (skewness) of the ion current density are computed for four average densities (Fig. 5). The

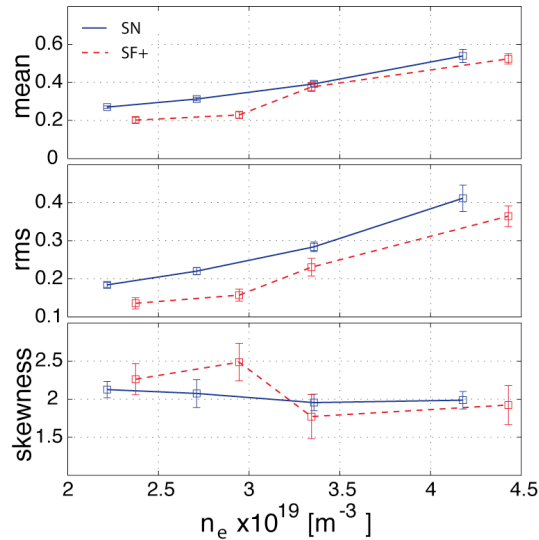


FIG. 5: Moments of the ion saturation current density  $J_{sat}$  for different plasma densities for SN (solid) and for SF+ (dashed). Squares correspond to the average value between probes #1-#3.

average and the r.m.s. values increase with the density while the skewness, which is a measure of the intermittency, stays almost constant at a high level. Moreover, the level of fluctuations is significantly lower for the SF+ configuration compared to the SN one, which seems to indicate that large amplitude blobs are less frequent two centimeters away from the LCFS in the SF+ configuration. Two reasons might be invoked to explain this observation: either blobs are convected faster to the strike points in the SF+ than in a SN configuration and therefore do not have time to reach the wall or, since the magnetic shear is larger for the SF+ plasma, blobs are more efficiently sheared-off and then dissipated. Additional measurements with a fast framing camera are under way and will confirm these hypotheses. The conditional sampling technique is a powerful tool to isolate coherent features between spatially separated measurements points [9]. The technique is applied to  $J_{sat}$  signals from probes #1-#4 for the lower and higher densities. Probe #2 is chosen as reference and the threshold for blob selection is set to  $6\sigma$ , where  $\sigma$  is the standard deviation. Even with such a large threshold, about 150 blobs are detected in a 300 ms long time trace. Results are summarized on Fig. 6. The auto conditional sampling for signal from probe #2 gives an insight of the average blob shape in time. It is rather short ( $\sim 30 \mu s$ ) and its asymmetric shape in time is more pronounced at high density and for the SF+ configuration. For both configurations and at low density, the blob is seen about  $20 \mu s$  earlier on probe #1 and about  $20 \mu s$  later on probe #3 with respect to the reference probe as indicated with the vertical dashed lines in Fig. 6 a-b). This observation indicates that blobs do not only propagate in the radial direction but also in both toroidal and poloidal directions. At higher density, no more correlation is observed between probes suggesting a high level of blob dissipation. These preliminary results seem to indicate that few differences are observed as far as statistical properties of blobs are concerned between SN and SF+ configurations at the LFS equatorial midplane, in L-mode. Nevertheless, larger differences could be expected at the second strike point and complementary measurements with LPs in an upper SF+ configuration will be performed.

### 3.2 ELM driven divertor target current in H-mode plasma with a snowflake divertor

Recently, ELMy H-mode regime has been achieved in the SF+ configuration in TCV and

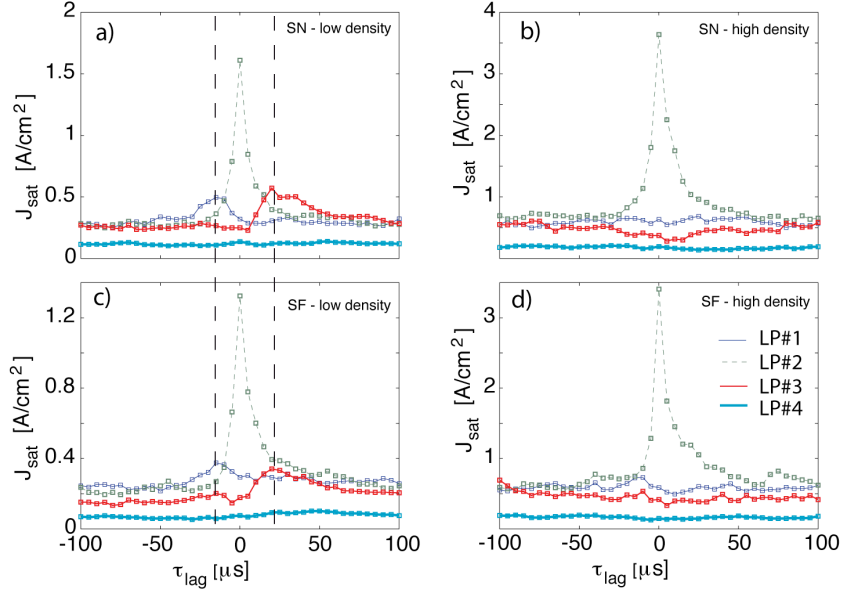


FIG. 6: Conditional sampling of  $J_{\text{sat}}$  for probes #1-#4 for the low density (left column) and for high density (right). The reference probe is LP#2.

compared to a SN plasma with similar shape [8]. The two configurations have a similar H-mode power threshold, whereas the SF+ confinement is 15% higher. The most striking difference is in the ELM frequency, reduced by a factor 2-3 in the snowflake, while the ratio of the energy lost per ELM to the plasma energy is only increased by 20-30%. Improved stability to kink-ballooning modes is consistent with this behaviour [10], although the ELM frequency variation cannot be quantitatively explained at present. For ELMy SN/SF+ plasmas, the target zone of several strike-points is monitored with Langmuir probes (LPs) during ELMs. Results are summarized in Fig. 7. The conditionally averaged  $J_{\text{sat}}$  is plotted as a function of time relative to the ELM crash detected on the  $D_{\alpha}$  signal and as a function of the distance relative to the strike point position. Despite the fact that it is impossible to estimate  $J_{\text{sat}}$  on the strike point at the ELM crash, one can nevertheless make some observations. First, the dynamics of the ELM cycle is shorter ( $\sim 3$  ms) for the SN configuration than for the SF+ one ( $\sim 5$  ms), which is consistent with the change of ELM frequency between both configurations. Secondly, although the strike points SP3 and SP4 are not directly connected to the main plasma, a significant  $J_{\text{sat}}$  is measured on these strike points indicating that the SF configuration may be a promising way to manage plasma exhausts in the SOL. The increase of  $J_{\text{sat}}$  on SP3 occurs about 1 ms after the ELM crash suggesting a complex mechanism of heat and particle transport at the main X-point. These results obtained with LPs are in line with measurements obtained with an Infrared camera, which have shown that a non-negligible fraction of the energy expelled during an ELM reaches the additional strike points in the snowflake configuration.

#### 4. Conclusions and outlook

The role of the plasma shaping on heat transport has been investigated from the point of view of turbulence level and correlation length. Electron temperature fluctuations have been measured using the correlation ECE diagnostic for different shapes ( $\delta = \pm 0.4$ ) in L-mode plasmas. At identical pressure profiles, the radial correlation length is divided by a factor two at negative triangularity compared with the positive case. This observation is compatible with existing local nonlinear simulations predicting a partial stabilization of the TEM turbulence

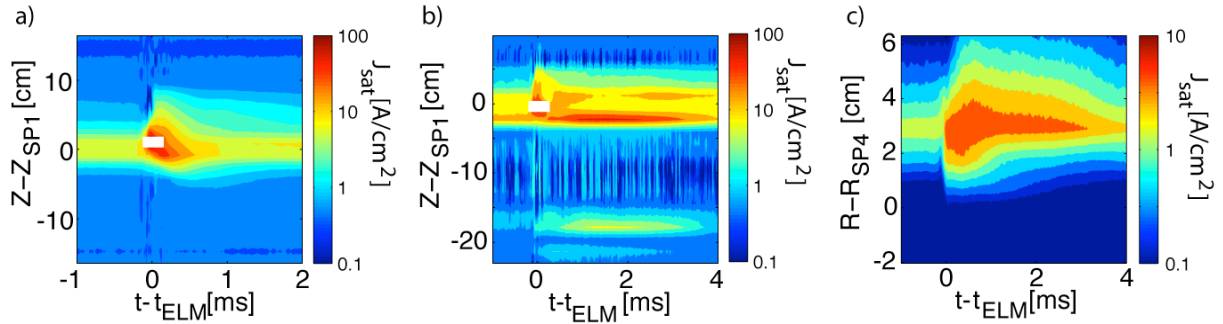


FIG. 7: 2D profiles of  $J_{sat}$  versus  $t-t_{ELM}$  for the target zone of SP1 a) in the SN configuration b) in the SF+ configuration and for the target zone of SP4 in SF+ configuration.

with triangularity. Nevertheless, a complete radial profile of the correlation length will reveal how deeply shaping effects are penetrating into the core. Results will be compared with global gyrokinetic simulations, which are underway. The snowflake divertor geometry has been extensively investigated in the last two years. Preliminary results on plasma edge properties measured with Langmuir probes have been reported. In L-mode plasmas, although the level of fluctuations is lower in SF+ SOL, the blob physics does not seem to be strongly affected with this configuration. In H-mode plasmas, a significant fraction of the power during an ELM crash is carried up to the additional strike points associated with the SF configuration. Measurements with LPs on the second strike point will help us in the understanding on how the power is shared between the divertor strike points. Finally, the SF- configuration for which the stability domain for ELMs is larger is currently explored in TCV.

*This work was supported in part by the Swiss National Science Foundation*

## References

- [1] POCHELON, A. et al., "Energy confinement and MHD activity in shaped TCV plasmas with localized electron cyclotron heating", Nucl. Fusion, **39** (1999) 1807
- [2] CAMENEN, Y. et al., "Impact of plasma triangularity and collisionality on electron heat transport in TCV L-mode plasmas", Nucl. Fusion **47** (2007) 510
- [3] MARINONI, A. et al., "The effect of plasma triangularity on turbulent transport: modeling TCV experiments by linear and non linear gyrokinetic simulations", Plasma Phys. Contr. Fusion **51** (2009) 055016
- [4] RYUTOV D. D. et al., "The magnetic field structure of a snowflake divertor", Phys. Plasmas **15**, (2008) 092501
- [5] PIRAS, F. et al., "Snowflake divertor plasmas on TCV", Plasma Phys. Control. Fusion **51** (2009) 055009
- [6] UDINTSEV, V.U. et al., "Recent Electron Cyclotron Emission results on TCV", Fus. Sci. Technol. **52** (2007) 161
- [7] PITTS, R. A. et al., "ELM driven divertor target currents on TCV", Nucl. Fusion **43** (2003) 1145
- [8] PIRAS, F. et al., "Snowflake H-mode in a tokamak plasma", Phys. Rev. Lett. **105**, (2010), 155003
- [9] JOHNSON H. et al., "Conditional eddies in plasma turbulence", Phys. Fluids **30**, (1987) 2239
- [10] S. Yu. Medvedev et al., "Edge Stability and Pedestal Profile Sensitivity of Snowflake Diverted Equilibria in the TCV Tokamak", Contrib. Plasma Phys. **50**, (2010) 324